Circadian Regulation of Lipid Mobilization in White Adipose Tissues

Anton Shostak,[1] Judit Meyer-Kovac,[1] and Henrik Oster[1,2]

In mammals, a network of circadian clocks regulates 24-h rhythms of behavior and physiology. Circadian disruption promotes obesity and the development of obesity-associated disorders, but it remains unclear to which extent peripheral tissue clocks contribute to this effect. To reveal the impact of the circadian timing system on lipid metabolism, blood and adipose tissue samples from wild-type, ClockΔ19, and Bmal1$^{-/-}$ circadian mutant mice were subjected to biochemical assays and gene expression profiling. We show diurnal variations in lipolysis rates and release of free fatty acids (FFAs) and glycerol into the blood correlating with rhythmic regulation of two genes encoding the lipolysis pacemaker enzymes, adipose triglyceride (TG) lipase and hormone-sensitive lipase, by self-sustained adipocyte clocks. Circadian clock mutant mice show low and nonrhythmic FFA and glycerol blood content together with decreased lipolysis rates and increased sensitivity to fasting. Instead circadian clock disruption promotes the accumulation of TGs in white adipose tissue (WAT), leading to increased adiposity and adipocyte hypertrophy. In summary, circadian modulation of lipolysis rates regulates the availability of lipid-derived energy during the day, suggesting a role for WAT clocks in the regulation of energy homeostasis. ***Diabetes*** **62:2195–2203, 2013**

Living organisms are influenced by rhythmic changes in the environment due to the Earth's rotation around its axis. In an attempt to optimally adapt to such recurring events, most species have evolved circadian clocks, internal timing systems controlling 24-h rhythms of behavior and physiology (1). In mammals, most, if not all, cells harbor their own molecular timer. Internal synchrony and thus overt behavioral and physiological rhythms are regulated via a hierarchical system of central and peripheral clocks. External time information is perceived by a master circadian pacemaker located in the hypothalamic suprachiasmatic nucleus, which relays timing cues to the rest of the body. In the suprachiasmatic nucleus and the periphery, the molecular clock machinery is based on interlocked transcriptional–translational feedback loops comprised of a set of clock genes. The basic helix–loop–helix transcription factors CLOCK and BMAL1 (ARNTL) induce expression of the negative regulators *Per1–3* and *Cry1/2* through binding to E-box promoter elements. With a delay of several hours, PER/CRY protein complexes enter the nucleus and repress activity of CLOCK/BMAL1 heterodimers, thereby shutting down their own transcription. Further loops interact with this E-box–mediated transcription rhythm and stabilize its characteristic 24-h periodicity. Clock genes further regulate the activity of numerous tissue-specific output genes, thereby translating time-of-day information into physiologically meaningful signals (2).

Both rodent and human studies suggest a tight interaction between circadian clock regulation and energy homeostasis. Circadian disruption, either external (as seen for example in shift workers) or internal (e.g., in *Clock* gene mutant mice), can lead to obesity and the development of type 2 diabetes and metabolic syndrome (3–6). While appetite regulation appears mostly centrally controlled, recent animal studies indicate an additional role for peripheral tissue clocks in the control of energy metabolism. For instance, local circadian oscillators in liver and pancreas regulate glucose utilization, whereas cardiomyocyte clocks are involved in cardiac repolarization (6–8).

White adipose tissues (WATs) store large amounts of lipids in the form of triglycerides (TGs). During extended periods of energy shortage (e.g., fasting), the release of lipids from WAT mediated by the hydrolysis of TGs to free fatty acids (FFAs) and glycerol (lipolysis) becomes an important energy source for other organs. The timing of FFA release from adipose stores, however, has to be tightly controlled, as excess of circulating lipids may lead to lipotoxicity and promote cardiovascular disorders (9). In contrast, redundant deposition of TGs causes obesity, a risk factor for type 2 diabetes. Previous reports show that adipose tissues exhibit rhythmic clock gene expression in mice and man (10–12). Cell-based and animal studies suggest that clock genes are positive regulators of adipogenesis (13,14). It remains unclear, however, how circadian disruption may lead to increased adipose tissue deposition and obesity, as observed in human shift workers and in various clock gene mutant mice.

In this study, we analyze the role of white adipose clocks in lipid utilization in mice. We show that self-sustained local clocks regulate rhythmic FFA release from WAT stores, thus revealing a novel and peripherally regulated mechanism by which circadian disruption may impinge on energy homeostasis.

RESEARCH DESIGN AND METHODS

Experimental animals. Male wild-type (C57BL/6), congenic homozygous *Clock*$^{\Delta 19}$ (15), *Bmal1*$^{-/-}$ (16), and *PER2::LUCIFERASE* (17) mice of 2–4 months of age were used for all experiments. All animal experiments were done after ethical assessment and licensed by the Office of Consumer Protection and Food Safety of the State of Lower Saxony and in accordance with the German Law of Animal Welfare. Mice were housed in small groups of five or fewer under a 12-h light/12-h dark cycle (LD) or constant darkness (DD) conditions with food and water access ad libitum.

Fat pad cultures. Wild-type or *PER2::LUCIFERASE* mice (17) were LD entrained and killed by cervical dislocation at Zeitgeber time (ZT) 9 (i.e., 3 h

From the [1]Circadian Rhythms Group, Max Planck Institute for Biophysical Chemistry, Göttingen, Germany; and the [2]Medical Department I, University of Lübeck, Lübeck, Germany.
Corresponding author: Henrik Oster, henrik.oster@uksh.de.
Received 20 October 2012 and accepted 17 February 2013.
DOI: 10.2337/db12-1449
This article contains Supplementary Data online at http://diabetes.diabetesjournals.org/lookup/suppl/doi:10.2337/db12-1449/-/DC1.

See accompanying commentary, p. 2175.

before lights off). WAT and brown adipose tissue (BAT) samples were isolated and washed with 1× Hanks' balanced salt solution (PAA Laboratories, Cölbe, Germany). Tissues were divided into 20–30-mg pieces and cultured in colorless Dulbecco's modified Eagle's medium (DMEM; PAA Laboratories) supplemented with 10% FBS (PAA Laboratories) and 100 nmol/L luciferin sodium salt (Biosynth, Staad, Switzerland). For RNA extraction fat pads were removed at 6-h intervals, and total RNA was extracted and processed as described below. Bioluminescence recordings were performed using a Lumicycle luminometer (Actimetrics, Willmette, IL). Period and damping rate were calculated using the Lumicycle Analysis software (Actimetrics).

Quantitative real-time PCR. Mice were entrained to LD for at least 2 weeks, released into DD, and killed at 37, 43, 49, 55, and 61 h after lights off (corresponding to circadian times 1, 7, 13, and 19, respectively). For LD cohorts, mice were kept under LD and killed at ZT1, 7, 13, and 19. Epididymal fat was isolated, and total RNA was extracted using TRIzol reagent (Life Technologies, Darmstadt, Germany). cDNA synthesis was performed by High Capacity cDNA Reverse Transcription Kit (Life Technologies) using random hexamer primers. Quantitative real-time PCR was performed using iQ SYBR Green Supermix on an CFX96 thermocycler (Bio-Rad, Munich, Germany) according to the manufacturer's protocol. Relative gene expression was quantified using a ΔΔ threshold cycle method and *Eef1α* as a reference gene (18). Primer sequences are listed in Supplementary Table 1.

Cloning of adipose TG lipase and hormone-sensitive lipase promoters and PCR mutagenesis. A 4.3-kb fragment containing the murine adipose TG lipase (*Atgl*) upstream sequence and the first intron were PCR-amplified from genomic DNA using Advantage 2 polymerase mix (Clontech, Mountain View, CA). PCR products were digested with *Hind*III (New England Biolabs, Ipswich, MA) and *Xho*I (New England Biolabs) and cloned into *Hind*III/*Xho*I–digested *pGL4* vector (Promega, Madison, WI). A 4.5-kb fragment of the murine hormone-sensitive lipase (*Hsl*) promoter was PCR-amplified as described for *Atgl*. PCR products were cloned into the *pGL3* vector by In-Fusion Cloning (Clontech). Inserts were confirmed by sequencing. E-box mutations to GGATCC were performed using a PCR mutagenesis kit (Agilent Technologies, Santa Clara, CA) and confirmed by sequencing. Primer sequences are listed in Supplementary Table 2.

Luciferase promoter assays. HEK293A and NIH-3T3 cells were maintained in DMEM (PAA Laboratories) supplemented with 10% FBS (PAA Laboratories) and antibiotics. One day prior to transfection, cells were plated onto 24-well plates at a density of 10^5 cells/well. HEK cells were cotransfected using PEI (Sigma-Aldrich, Hamburg, Germany) and 50 ng of *pGL3/4* reporter plasmid in the presence of 200 ng of *Bmal1*, *Clock*, or *Cry1* constructs. Empty *pcDNA3.1* vector was used to make up the total amount of DNA to 0.7 μg/well. A total of 10 ng of a *pRL-CMV Renilla* luciferase reporter vector (Promega) was added to each reaction as internal control. Two days later, cells were harvested and assayed using the Dual-Luciferase Reporter Assay System (Promega) on a TriStar LB941 luminometer (Berthold Technologies, Wildbach, Germany). NIH-3T3 cells were transfected using X-fect (Clontech) with 1 μg *pGL3-Hsl*, *pGL4-Atgl*, or *Bmal1-luc* (19) reporter plasmids. Two days later, cells were synchronized by 50% serum shock for 2 h. For luminescence recordings, cells were kept in colorless DMEM, 10% FBS, and 100 nmol/L luciferin sodium salt (Life Technologies).

Chromatin immunoprecipitation. Epididymal fat pads from wild-type and *Bmal1*$^{-/-}$ mice were isolated at ZT7 and ZT19, homogenized, and immediately cross linked in 1% formaldehyde. Chromatin was sonicated to obtain an average DNA length of ~400 bp (15-s on/20-s off cycles for 22 min) using a Bioruptor (Diagenode Inc.). Samples were incubated overnight at 4°C with BMAL1 antibody (*N*-20; Santa Cruz Biotechnology). After clearing, samples were incubated with A/G agarose beads (Thermo Scientific) for 1 h at 4°C followed by intensive washings. Afterward, samples were boiled for 10 min in 10% Chelex (Bio-Rad) with Proteinase K (150 μg/mL) and spun down. DNA-containing supernatant was collected for PCR. Quantitative real-time PCR was performed as described above, and values were normalized to percentage of input. Primer sequences are listed in Supplementary Table 3.

Lipolysis assays. Epididymal fat pads from were dissected at the given time points, cut into 10–25 mg samples, and incubated at 37°C in DMEM and 10% FBS with antibiotics. Glycerol release was measured from media aliquots using Free Glycerol Reagent (Sigma-Aldrich) and normalized to fat pad dry weight.

Blood glycerol and FFA measurements. Trunk blood was collected at circadian times/ZT 1, 7, 13, and 19 and was allowed to clot. Subsequently serum was isolated by centrifugation at 2,000*g* for 20 min at 4°C. Serum FFAs, TG/glycerol, and cholesterol levels were determined using a NEFA kit (Zen-Bio, Research Triangle Park, NC), serum TG determination kit (Sigma-Aldrich), and cholesterol assay kit (Cayman Chemical) according to the manufacturers' protocols.

Adipocyte histology. Freshly isolated epididymal WAT samples were fixed with 4% paraformaldehyde/PBS overnight. Samples were dehydrated with ascending alcohol concentrations and embedded in paraffin. Sections were cut at 6 μm and stained with hematoxylin-eosin. Adipocyte size was determined with Image J software (National Institutes of Health, Bethesda, MD).

Statistical analysis. All results are expressed as a mean ± SEM. For statistical comparison unpaired two-tailed Student *t* tests or two-way ANOVAs with Bonferroni posttests were performed using Prism 5 software (GraphPad Software). Analysis of circadian gene expression was performed with CircWave software (20) downloaded at http://www.euclock.org. *P* values <0.05 were considered significant.

RESULTS

Circadian Clock$^{\Delta 19}$ mutants show increased adiposity and blunted FFA and glycerol rhythms in blood. To gain more insights into the circadian regulation of lipid metabolism, we compared diurnal profiles of various lipid parameters in serum between circadian clock–deficient *Clock*$^{\Delta 19}$ and wild-type mice. Consistent with a previous report (4), *Clock*$^{\Delta 19}$ mice had significantly higher cholesterol levels in the blood, albeit no significant circadian variation was observed in either genotype (Fig. 1*A*). In contrast, serum TG levels were rhythmic, but indistinguishable between genotypes (Fig. 1*B*). Interestingly, FFA serum levels showed a robust circadian profile in wild-type animals ($P = 0.005$). This rhythm was abolished, and overall levels were decreased in *Clock*$^{\Delta 19}$ mutants ($P = 0.802$) (Fig. 1*C*), suggesting an involvement of the circadian clock machinery in the regulation of fatty acid release from TG stores. In line with this hypothesis, serum glycerol concentrations showed similar variations in wild-type serum, whereas in *Clock*$^{\Delta 19}$ mutants, levels were nonrhythmic and overall low ($P = 0.003$ vs. $P = 0.678$) (Fig. 1*D*). Comparable effects on FFA and glycerol levels were also observed under LD conditions (Fig. 1*E* and *F*) and in another clock-deficient mouse model, *Bmal1*$^{-/-}$ (Fig. 1*G* and *H*). Surprisingly, while blood TG and FFA levels were unaltered or low, *Clock*$^{\Delta 19}$ mutants at the same time exhibited higher overall body weight gain with increased adiposity (Fig. 2*A* and *B* and Supplementary Fig. 1*A*) together with hyperphagy, but unaltered overall activity (Supplementary Fig. 1*B* and *C*) (4). Histological analysis of WAT paraffin sections revealed increased WAT lipid accumulation and adipocyte hypertrophy in *Clock*$^{\Delta 19}$ mutant mice (Fig. 2*C*), suggesting that the *Clock* mutation either promotes lipid accumulation or inhibits lipid mobilization in WAT.

Circadian regulation of genes involved in WAT lipid metabolism. Circadian clocks regulate local cellular physiology via transcriptional programs involving large numbers of tissue-specific clock-controlled genes (21). To test if molecular clocks are involved in regulating WAT physiology, we analyzed circadian variations in mRNAs of genes involved in WAT lipid metabolism. Genes were selected using the Gene Ontology database (http://www.geneontology.org) and expression data assembled on BioGPS (http://biogps.org) and compared with published literature (Supplementary Fig. 2*A*). Epididymal WAT transcript levels were assessed at the beginning of the rest phase (37 h in DD) and in the early subjective night (49 h in DD). For genes which showed significant regulation between both time points, we determined full circadian transcriptional profiles in *Clock*$^{\Delta 19}$ and wild-type mice. Of the genes associated with FFA transport and TG biosynthesis (i.e., the conversion of FFAs for storage in adipose lipid droplets), *Caveolin2*, the acyl-CoA synthetases *Acsl1* and *Acsl4* and the phosphatidate phosphatase *Lpin1* showed significant differences in expression between

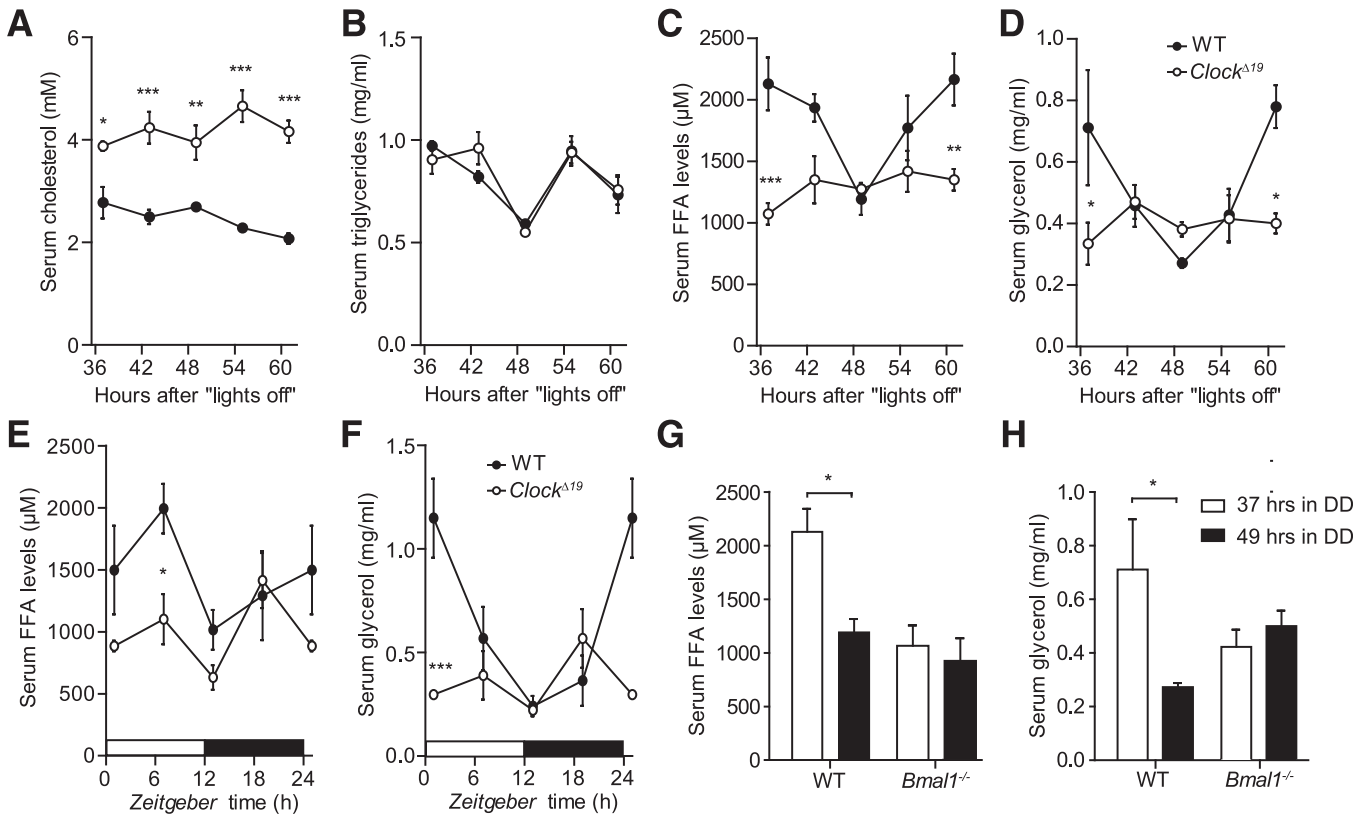

FIG. 1. Serum lipids change in *Clock*$^{\Delta 19}$ mice. Diurnal profiles of cholesterol (*A*), TGs (*B*), FFAs (*C*), and glycerol (*D*) in the serum of wild-type (WT; closed circles) and *Clock*$^{\Delta 19}$ (open circles) mice in DD (n = 3/time point). Time points indicate hours spent in DD after the last lights off. Diurnal profiles of FFAs (*E*) and glycerol (*F*) in the serum of wild-type (closed circles) and *Clock*$^{\Delta 19}$ (open circles) mice in LD conditions (n = 3–5/time point). Time-of-day dependent variations in serum FFA and glycerol levels in WT (black bars) and *Bmal1*$^{-/-}$ (white bars) animals kept in DD (n = 3–5/time point). All data are shown as means ± SEM. *P < 0.05; **P < 0.01; ***P < 0.001 by two-way ANOVA with Bonferroni posttest.

37 and 49 h in DD (Fig. 3*A*). In *Clock*$^{\Delta 19}$ mutants, FFA transport/TG biosynthesis mRNAs were either unaffected (*Acsl4*, *Lpl*) or dampened and overall downregulated when compared with wild-type controls (Fig. 3*B* and *C* and Supplementary Fig. 2*B*). In contrast, the mRNAs of two rate-limiting lipolytic enzymes, *Atgl* (or *Pnpla2*) and *Hsl* (or *Lipe*), exhibited circadian variations in wild-type animals (Fig. 3*A*), while in *Clock*$^{\Delta 19}$ mutants, *Atgl* and *Hsl* mRNA levels (together with that of *Mgll*) were significantly reduced and arrhythmic (Fig. 4*A*) ($P < 0.001$ vs. $P = 0.85$ [*Atgl*] and $P < 0.001$ vs. $P = 0.63$ [*Hsl*], respectively), strongly correlating with the reduced and arrhythmic FFA/glycerol serum levels observed in these mice (Fig. 1). To test TG breakdown from WAT stores more directly, we performed lipolysis assays on fat pad explants at four different time points in DD and LD. In wild-types, glycerol excretion showed a rhythmic pattern, whereas dampened rhythmicity and a general downregulation of basal lipolysis rates were observed in explants of *Clock*$^{\Delta 19}$ mice (Fig. 4*B* and *C*) ($P = 0.001$ vs. $P = 0.95$ [DD] and $P < 0.001$ vs. $P = 0.63$

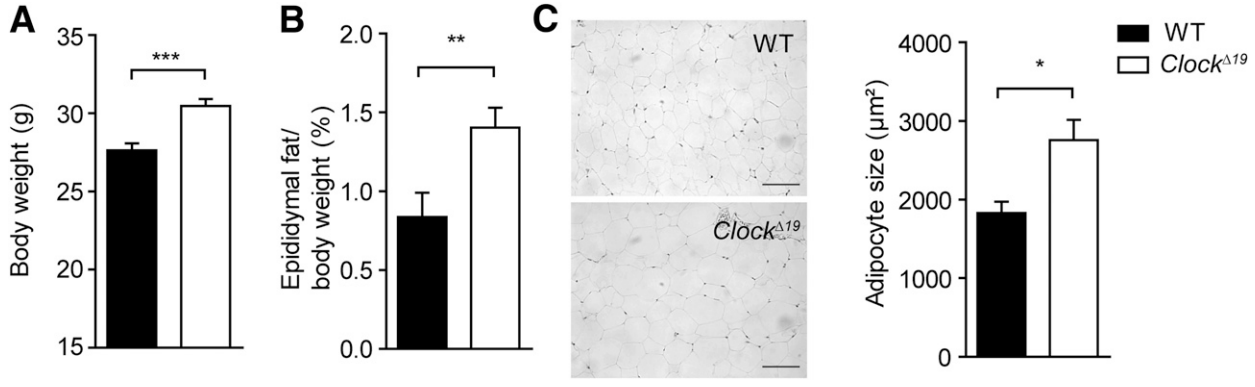

FIG. 2. Increased body weight and adiposity in *Clock*$^{\Delta 19}$ mice. Body weight (*A*) and adiposity (epididymal fat to body weight ratio) (*B*) in wild-type (WT; black bars) and *Clock*$^{\Delta 19}$ (white bars) mice fed standard chow for 10 weeks (n = 14). *C*: Representative sections and adipocyte size of epididymal WAT after 10 weeks of standard diet (scale bars, 100 μm; n = 3). *P < 0.05; **P < 0.01; ***P < 0.001 by unpaired t test. All data are shown as means ± SEM.

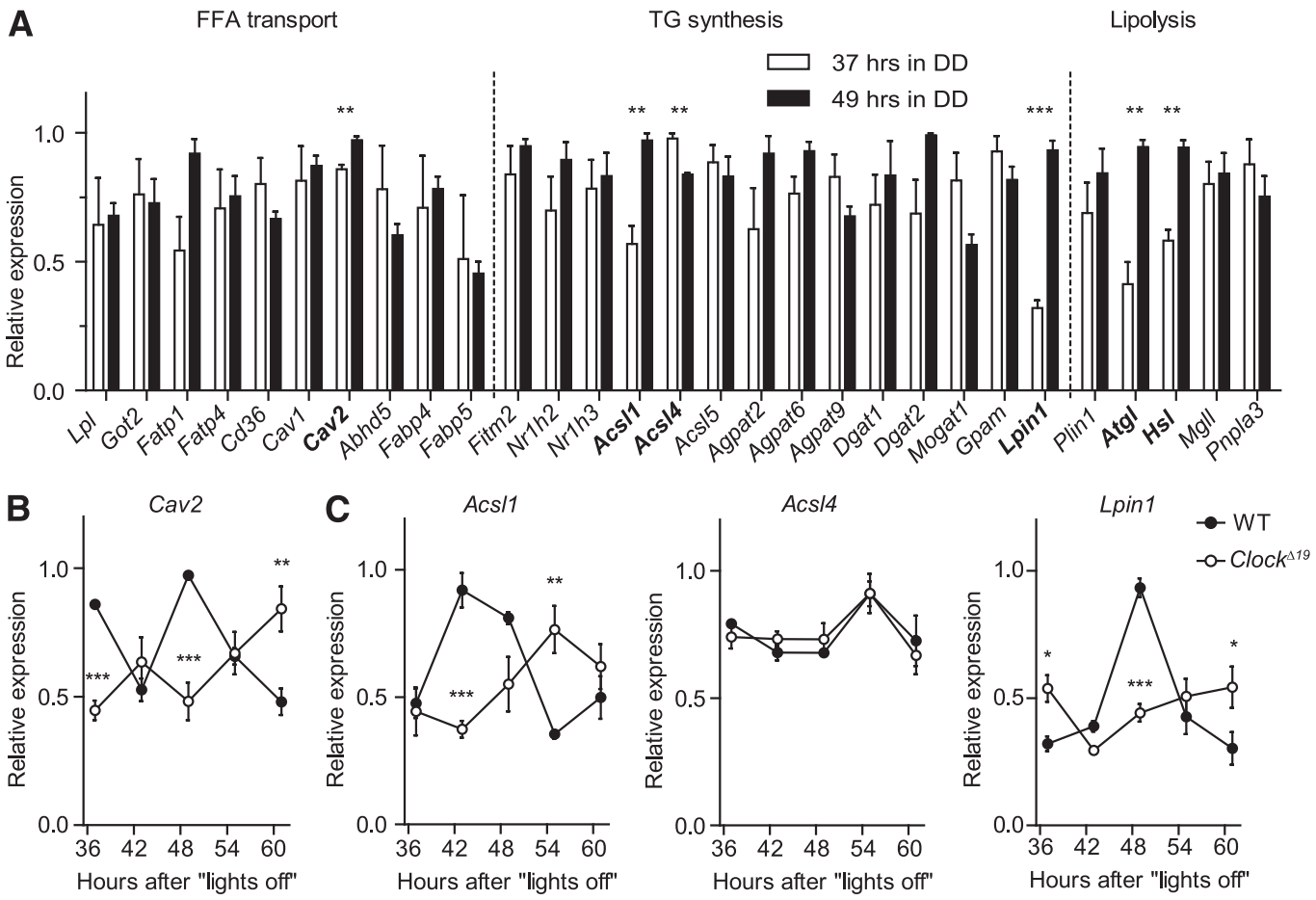

FIG. 3. Circadian clock controls TG metabolism in WAT. *A*: mRNA levels of genes involved in adipocyte TG metabolism from wild-type (WT) WAT samples isolated at two opposite circadian time points, 37 h (open bars) and 49 h (closed bars) in DD (n = 3 per time point [*$P < 0.05$; **$P < 0.01$ by unpaired t test]). Circadian expression profiles of candidate genes from (*A*) involved in FFA transport (*B*) and TG synthesis (*C*) in WAT samples from WT (closed circles) and *Clock*$^{\Delta 19}$ (open circles) mice in DD (n = 3/time point [*$P < 0.05$; **$P < 0.01$; ***$P < 0.001$ by two-way ANOVA with Bonferroni posttest]). All data are shown as means ± SEM.

[LD], respectively). Of note, on the second day in DD, *Clock* mutants retained a rhythmic, though dampened, feeding profile (Supplementary Fig. 3*A*). Moreover, when animals were subjected to nighttime restricted feeding (i.e., food access between ZT12 and ZT24) under LD conditions, daytime *Atgl* and *Hsl* levels remained reduced in *Clock* mutant mice, indicating that *Atgl/Hsl* transcription does not merely reflect feeding rhythms (Supplementary Fig. 3*B*). Analogously, *Bmal1*$^{-/-}$ mice showed lower expression levels of *Atgl* and *Hsl* (Fig. 4*D*) and *Bmal1*-deficient fat pads displayed lower lipolysis rates (Fig. 4*E*)

Adipose peripheral clocks regulate rhythmic expression of *Atgl* and *Hsl*. To further characterize the circadian regulation of adipose physiology, we analyzed WAT clock gene regulation in DD. Expression of *Bmal1*, *Per2*, and *Dbp* genes exhibited robust circadian variations in wild-type animals, which were significantly downregulated and arrhythmic (*Per2*, *Dbp*) or dampened (*Bmal1*) in *Clock*$^{\Delta 19}$ mutant mice (Fig. 5*A*). To characterize the sustainability of molecular circadian rhythms in WAT and compare clock function between different fat depots, we cultured epididymal, perirenal, peritoneal, subcutaneous white, as well as intrascapular BAT fat explants from *PER2::LUCIFERASE* circadian reporter mice. All cultures showed sustained bioluminescence rhythms in the circadian range for several days (Fig. 5*B* and Supplementary Fig. 4*A*) (17). The phases of luminescent oscillations were comparable between different depots and to those reported from other peripheral tissue explants (17,22) (Supplementary Fig. 4*B*). Periodogram analysis revealed endogenous periodicities of ~25 h; statistically significant differences in period were only observed between epididymal white fat and BAT (25.8 ± 0.2 vs. 24.7 ± 0.3 h; Supplementary Fig. 4*C*). Moreover, rhythm dampening was comparable among all adipose tissues tested (Supplementary Fig. 4*D*). To test if *Atgl* and *Hsl* transcription is clock-driven at the tissue level, we kept epididymal fat explants in culture for 36 h. We observed rhythmic *Atgl* and *Hsl* mRNA expression in wild-type fat pads ($P < 0.001$ and $P = 0.006$, respectively). Similar to what was observed in vivo, transcript variations were abolished, and overall levels were reduced in explants from *Clock*$^{\Delta 19}$ mice ($P > 0.8$ for both genes) (Fig. 5*C*). Notably, the expression rhythms of the two lipolytic genes were in phase coherence with E-box–regulated genes such as *Per2* and in antiphase to *Bmal1* (compare Fig. 5*C* and *D*). Taken together, these data suggested a direct control of *Atgl* and *Hsl* expression by CLOCK and BMAL1.

BMAL1 and CLOCK regulate expression of *Atgl* and *Hsl* via E-boxes. We identified two canonical E-box sequences (CACGTG) in the first intron of *Atgl* (chr7:

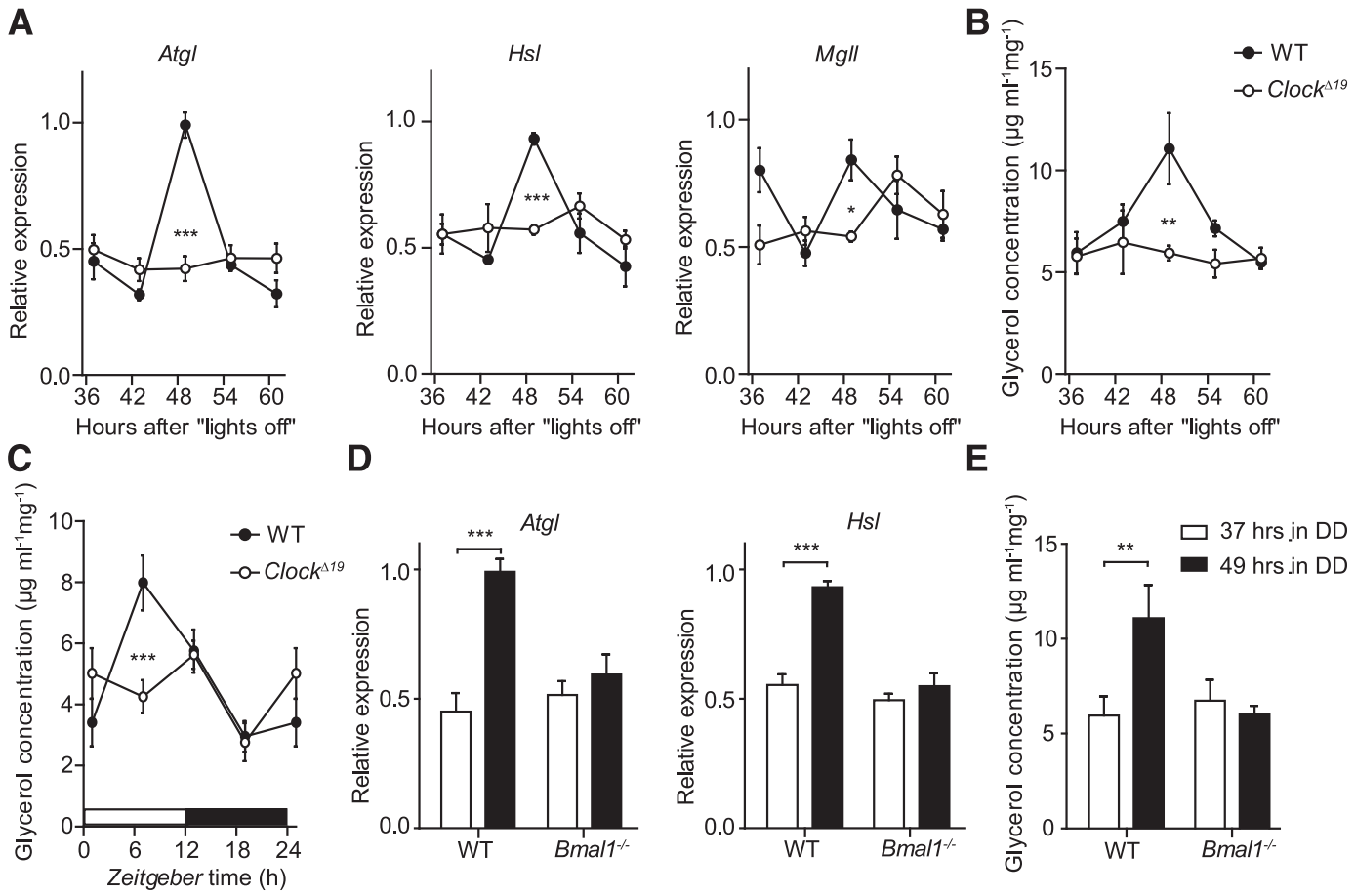

FIG. 4. Circadian clock regulates lipid mobilization in WAT. *A*: Circadian expression profiles of genes involved in lipolysis in adipose tissue from wild-type (WT; closed circles) and *Clock*$^{\Delta 19}$ (open circles) mice in DD (n = 3–4/time point). Profiles of glycerol excretion from WT (closed circles) and *Clock*$^{\Delta 19}$ (open circles) epididymal WAT fat-pad explants harvested in DD (*B*) and LD (*C*) (n = 6–14/time point). *D*: Expression of *Atgl* and *Hsl* in WAT of WT (black bars) and *Bmal1*$^{-/-}$ (white bars) animals at 37 and 49 h after lights off (n = 2–3/time point). *E*: Changes in glycerol excretion from WT (black bars) and *Bmal1*$^{-/-}$ (white bars) epididymal WAT fat-pad explants harvested at 37 and 49 h after lights off (n = 8/time point). All data are shown as means ± SEM. *P < 0.05; **P < 0.01; ***P < 0.001 by two-way ANOVA with Bonferroni posttest.

148642099–148642104, 148642860–148642866) and in the upstream region of *Hsl* (chr7: 26181156–26181161, 26181424–26181430). Genomic DNA fragments containing these *cis*-regulatory elements were used for luciferase-based transactivation assays in HEK293A cells (Fig. 6*A*). Cotransfection with *Clock* and *Bmal1* increased the activity of both *Atgl* and *Hsl* promoters by 6.5- and 2.3-fold, respectively (Fig. 6*B*). Activation was inhibited by cotransfection with *Cry1*, a negative E-box regulator. Moreover, mutation of the E-box proximal to the second exon of the *Atgl* gene (chr7: 148642860–148642866) abolished transcriptional activation by CLOCK/BMAL1 (Fig. 6*B*, *left*). Similar results were obtained upon mutation of both upstream E-boxes in the *Hsl* promoter (Fig. 6*B*, *right*). To confirm direct BMAL1 promoter binding in vivo, we performed chromatin immunoprecipitation (ChIP) on epididymal adipose tissue sampled at two different time points. ChIP analysis revealed time-of-day dependent occupancy of BMAL1 on *Dbp*, *Atgl*, and *Hsl* E-boxes, but not on 500-bp downstream regions in wild-type mice. In *Bmal1*-deficient animals, binding signal was markedly reduced (Fig. 6*C*). Finally, we transfected *Atgl-luc* and *Hsl-luc* constructs into NIH-3T3 cells and recorded bioluminescence for 48 h after serum shock synchronization. We observed a rhythmic bioluminescence signal for *Atgl-luc* and *Hsl-luc* antiphasic to *Bmal1-luc* (Supplementary Fig. 4*E* and *F*), comparable to what has been reported for other E-box controlled genes such as *Per2* (23). Together, these results strongly suggest that circadian *Atgl* and *Hsl* transcription is directly regulated by CLOCK/BMAL1 via E-box activation at the adipose tissue level.

Defective lipolysis leads to fasting intolerance in Clock$^{\Delta 19}$ mutant mice. Lipolysis becomes an important energy source during the fasting (i.e., rest) phase of the day. In line with this, reduced FFA mobilization provokes aberrant physiological responses under fasting conditions (24). To test if fasting responses are impaired in *Clock*$^{\Delta 19}$ mutants, we food-deprived mutant and wild-type mice starting at the end of the light phase (ZT12). FFA and glycerol levels were upregulated in serum in response to 12- and 24-h starves (starting at the end of the normal rest phase, at ZT12) in wild-types, whereas the lipolytic response was severely dampened in *Clock*$^{\Delta 19}$ animals (Fig. 7*A* and *B*). Given that FFA release, and, thus, the availability of lipids as energy source, appeared impaired, we speculated that under fasting conditions, mutants may rely more heavily on carbohydrate or protein utilization (24). In line with this, liver glycogen stores in *Clock*$^{\Delta 19}$ mice were depleted much faster than in wild-types under fasting conditions (Fig. 7*C*). Moreover, after food removal, mutants showed lower rectal temperature when compared

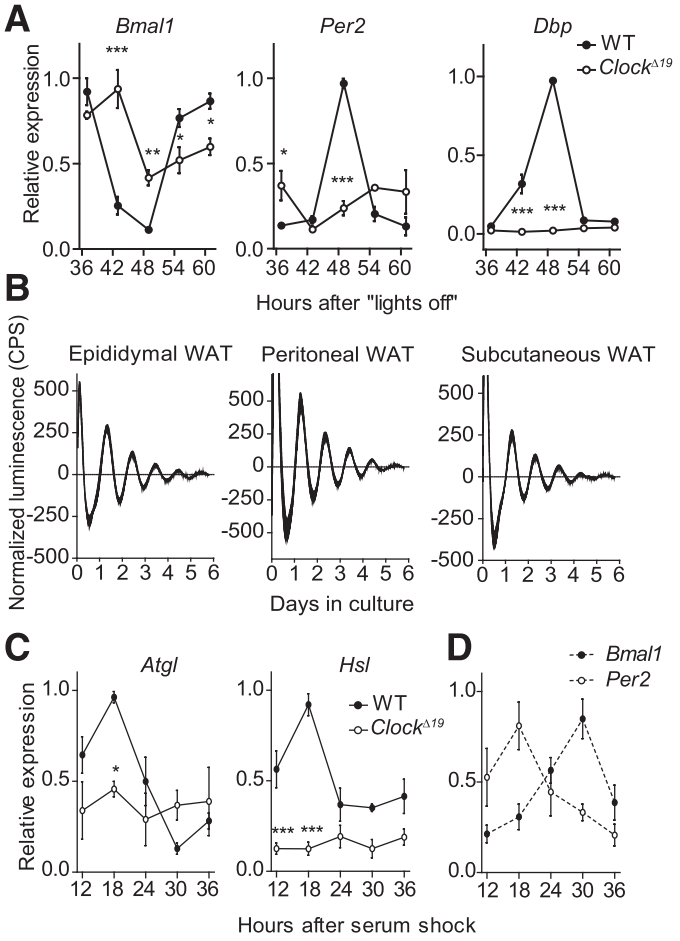

FIG. 5. Local WAT clocks regulate expression of *Atgl* and *Hsl*. *A*: Expression profiles of *Bmal1*, *Per2*, and *Dbp* mRNAs in WAT of wild-type (WT; closed circles) and *Clock*$^{\Delta 19}$ (open circles) mice in DD (n = 3/time point). *B*: Representative baseline-subtracted luminescence recordings from epididymal, peritoneal, and subcutaneous WAT explants of *PER2::LUCIFERASE* circadian reporter mice. *C*: Rhythmic expression of *Atgl* and *Hsl* transcripts in WT (closed circles), but not *Clock*$^{\Delta 19}$ (open circles), cultured fat-pad explants (n = 3/time point). *D*: Antiphasic expression of *Per2* (open circles) and *Bmal1* (closed circles) mRNAs in cultured WT fat-pad explants (n = 3/time point). All data are shown as means ± SEM. *P < 0.05; **P < 0.01; ***P < 0.001 by two-way ANOVA with Bonferroni posttest. CPS, counts per second.

with wild-type controls, implying decreased thermogenesis due to general energy shortage (Fig. 7*D*).

DISCUSSION

Circadian physiological rhythms are generated by interplay between systemic time cues (e.g., rhythmic hormones or metabolites) and the orchestration of transcriptional programs by local tissue oscillators. As a result many physiological parameters that exhibit diurnal variations are altered in mice with perturbed molecular clocks (5,6). In this article, we report that blood FFA and glycerol concentrations show strong variations across the day. This rhythm appears to not merely reflect rhythmic food intake and seems to critically depend on the presence of functional CLOCK/BMAL1. Moreover, in humans, it has been shown that FFA and glycerol are still rhythmic under constant routine conditions (25). During fasting conditions (e.g., during the daily rest phase), adipose-released FFAs become an important energy source (26,27). Therefore, the mobilization of FFAs may be critically involved in the regulation of metabolic homeostasis.

In line with previous studies in rats (28,29), we showed circadian rhythms in baseline WAT lipolysis rates and FFA levels in the blood of wild-type mice. In *Clock*$^{\Delta 19}$ and *Bmal1*$^{-/-}$ mutants, both rhythms were flattened and downregulated [our data and (30,31)], indicating defects in lipid mobilization. In agreement with this, it has previously been demonstrated that young *Bmal1*$^{-/-}$ mice show increased adiposity (8,32,33), while C57BL/6 *Clock*$^{\Delta 19}$ animals are obese and are more sensitive to high-fat diet (4). Rhythmic clock gene expression has been detected in many tissues in rodents and humans including various adipose depots (10–12). Using *PER2::LUCIFERASE* fat-pad explants cultures, we showed that adipose clocks display similar endogenous rhythm sustainment as described for other peripheral oscillators. We identified *Atgl* and *Hsl*, which encode for two lipolysis pacemaker enzymes responsible for >95% of TG hydrolysis activity (34), as targets of the local WAT clock machinery. *Atgl/Hs*l transcriptional rhythms were accompanied by rhythmic lipolytic activity in explant cultures and rhythmic elevation of the lipolysis products FFAs and glycerol in the blood. Of note, increased *Atgl/Hsl* mRNA expression preceded the elevation of lipolytic products in the blood of wild-type animals by several hours, probably reflecting a delay between the initiation of the lipolytic response and the emergence of a measurable physiological effect. This delay results in high glycerol and FFA levels during the rest phase when both are used for energy production. *Hsl*-deficient mice show hypertrophic adipocytes, reduced lipolysis rates, and decreased FFA levels, though their body weight is normal (35). *Atgl* conventional and adipocyte-specific mutants display the same phenotype together with increased body weight (36–39). Although the precise mechanism by which impaired lipolysis contributes to the development of obesity is not well-understood, cell-based studies suggest that reduced expression of *Atgl* and *Hsl* leads to TG accumulation in lipid droplets in adipocytes (40,41). Consistent with this hypothesis, our data suggest that dampened circadian lipolysis rhythms, as seen in *Clock* and *Bmal1* mutant mice, may promote TG accumulation in WAT. Moreover, reduced availability of FFAs as peroxisome proliferator–activated receptor cofactors may disrupt oxidative metabolism in mitochondria in other organs (39,42). Of note, expression of both enzymes was reported to be decreased in adipose tissue in obesity, thus leaving a possibility that downregulation of *Atgl* and *Hsl* transcript levels in *Clock*$^{\Delta 19}$ and *Bmal1*$^{-/-}$ animals might be rather the consequence than the cause of their adiposity. Our in vitro data suggest that *Atgl* and *Hsl* are direct targets of CLOCK/BMAL1, independent of metabolic state, but further studies are needed to clarify the impact of body weight and composition in this context (43,44). Moreover, we cannot exclude that disrupted feeding rhythms in *Clock*$^{\Delta 19}$ (Supplementary Fig. 2) mice may impinge on lipolysis rates via hormonal regulation (e.g., via leptin or insulin, which are known to induce and inhibit lipolysis, respectively) (45,46). However, circadian feeding profiles were not totally arrhythmic in *Clock* mutant mice, and *Atgl/Hsl* expression remained dampened in rhythmically fed *Clock* mutants. Further, reduced pancreatic secretion of insulin and hyperleptinemia have been reported in *Clock*$^{\Delta 19}$ mice (4,6), both of which appear insufficient to restore blood FFA and glycerol levels.

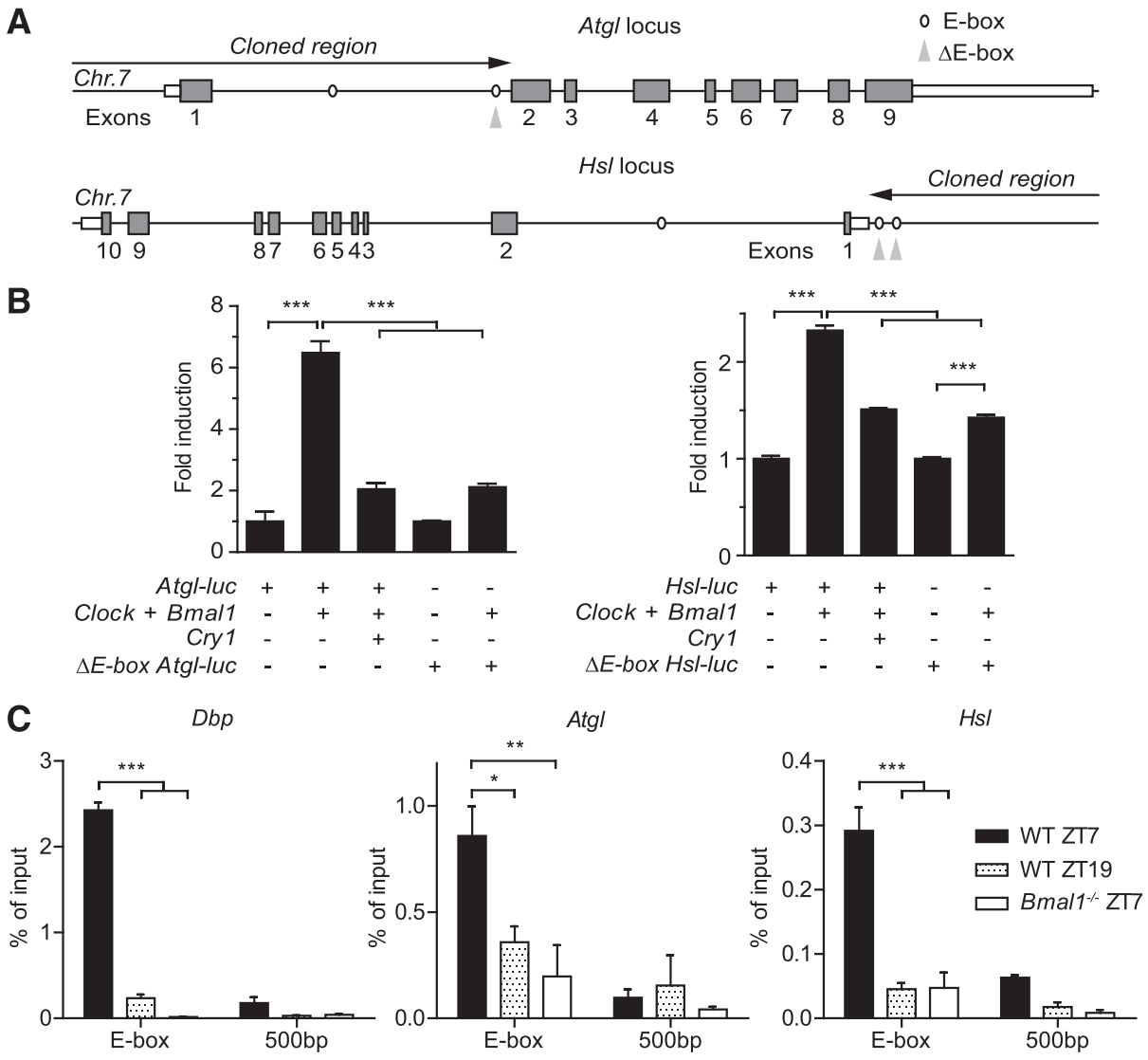

FIG. 6. CLOCK and BMAL1 drive rhythmic transcription of *Atgl* and *Hsl* via E-boxes. *A*: Maps of the 5′ regions of the genomic loci of murine *Atgl* (*top*) and *Hsl* (*bottom*) on chromosome 7 (*Chr.7*). Putative E-box enhancers are indicated by ovals. Black arrows depict the genomic sequences cloned for promoter studies. Mutated E-boxes are indicated by gray arrowheads. *B*: Luciferase reporter assays in HEK293 cells for wild-type (WT) and mutated *Atgl* (*left*) and *Hsl* (*right*) promoters in response to cotransfection with *Clock/Bmal1* and *Cry1* (n = 3; ***P < 0.001 by one-way ANOVA with Bonferroni posttest). C: Time-dependent BMAL1 binding to *Dbp*, *Atgl*, and *Hsl* E-boxes and 500-bp downstream regions as identified by ChIP in WAT (n = 3/time point [*P < 0.05; **P < 0.01; ***P < 0.001 by two-way ANOVA with Bonferroni posttest]). All data are shown as means ± SEM.

Instead, our results argue that rhythmic lipolysis is, at least in part, locally controlled by adipose circadian clocks. In line with this, oscillations of *Atgl* and *Hsl* mRNAs are sustained in fat pad explants ex vivo. Reporter gene and ChIP assays further indicate that CLOCK/BMAL1 directly and rhythmically bind to E-boxes in the promoters of *Atgl* and *Hsl*.

Mice with defective lipolysis exhibit impaired metabolic compensation during food deprivation (24). Consistently, our data reveal that $Clock^{\Delta 19}$ mutants show aberrant fasting responses. Once external energy supplies are disrupted, glycogen stores become quickly depleted, while mice are unable to fully engage their lipid stores in WAT to deliver further energy for maintaining stable body temperature. Alternatively, the development of brown adipocytes may be affected in $Clock^{\Delta 19}$ mice, or the $Clock^{\Delta 19}$ mutation may directly impair brown adipose thermogenesis (11,39).

During the inactive phase, wild-type mice switch their energy substrate preference to lipids, which corresponds to a lower respiratory exchange ratio (47). *Hsl*- and *Atgl*-deficient animals, however, continue to primarily use carbohydrates during that time due to impaired FFA release into the blood (38). Remarkably, a similar respiratory exchange ratio phenotype was described for $Clock^{-/-}$ and $Bmal1^{-/-}$ mice (48,49), which, as our data suggest, could be explained by impaired lipid use. In contrast, animals lacking the transcriptional repressor and negative regulator of *Bmal1* REV-ERBα (NR1D1) show increased expression of both *Clock* and *Bmal1* and use lipids as the predominant energy source through their efficient FFA mobilization and membrane transport (50).

So far, the mechanistic link between circadian disruption and associated metabolic defects is not clearly understood. In this study, we show that adipose-tissue clocks may directly affect diurnal lipid homeostasis by

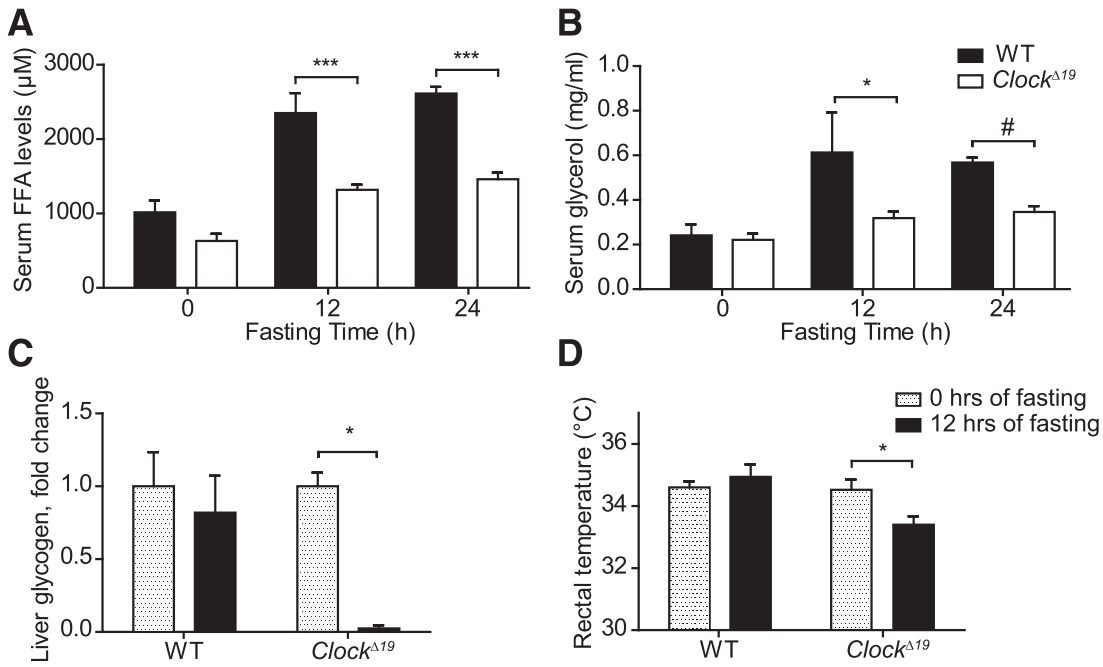

FIG. 7. Aberrant fasting responses in $Clock^{\Delta 19}$ mice. Serum FFA (*A*) and glycerol (*B*) levels after 12 and 24 h of food deprivation in wild-type (WT; closed bars) and $Clock^{\Delta 19}$ (open bars) mice (n = 3–5/time point). *C*: Normalized changes in liver glycogen content of WT and $Clock^{\Delta 19}$ mice during 12-h fasting (n = 3 to 4). *D*: Rectal temperature in WT and $Clock^{\Delta 19}$ animals during 12-h fasting (n = 6–12). All data are shown as means ± SEM. *$P < 0.05$; ***$P < 0.001$ by two-way ANOVA with Bonferroni posttest; #$P < 0.001$ by unpaired t test.

regulating FFA/glycerol mobilization from WAT stores via transcriptional regulation of the lipolytic machinery. By this, adipocyte clock function may directly impinge on energy homeostasis, thus representing a potential new target for pharmacological resetting of circadian physiology (51,52). Based on the evidence obtained from $Clock^{\Delta 19}$ and $Bmal1^{-/-}$ mice, we suggest that impaired lipid mobilization may lead to an imbalance in energy homeostasis, promoting increased adiposity. It remains to be clarified, however, to which extent WAT lipolysis defects contribute to the obese phenotype seen in $Clock^{\Delta 19}$ mutant mice since other alterations such as changed feeding patterns may further promote the development of obesity after circadian disruption (4,53,54).

ACKNOWLEDGMENTS

A.S. is supported by the Max Planck Society. H.O. is an Emmy Noether Fellow of the Deutsche Forschungsgemeinschaft and a Lichtenberg Fellow of the Volkswagen Foundation.

No potential conflicts of interest relevant to this article were reported.

A.S. and H.O. planned the study, researched data, and wrote the manuscript. J.M.-K. researched data. H.O. is the guarantor of this work and, as such, had full access to all the data in the study and takes responsibility for the integrity of the data and the accuracy of the data analysis.

The authors thank Dr. Ana Martinez Hernandez (Max-Planck-Institute for Biophysical Chemistry, Göttingen, Germany) for critical reading of the manuscript, and Dr. Moritz Rossner (Max-Planck-Institute for Experimental Medicine, Göttingen, Germany) and Dr. Steve A. Brown (University of Zürich, Zürich, Switzerland) for providing DNA constructs.

REFERENCES

1. Harmer SL, Panda S, Kay SA. Molecular bases of circadian rhythms. Annu Rev Cell Dev Biol 2001;17:215–253
2. Storch KF, Lipan O, Leykin I, et al. Extensive and divergent circadian gene expression in liver and heart. Nature 2002;417:78–83
3. Bray MS, Young ME. Circadian rhythms in the development of obesity: potential role for the circadian clock within the adipocyte. Obes Rev 2007; 8:169–181
4. Turek FW, Joshu C, Kohsaka A, et al. Obesity and metabolic syndrome in circadian Clock mutant mice. Science 2005;308:1043–1045
5. Rudic RD, McNamara P, Curtis AM, et al. BMAL1 and CLOCK, two essential components of the circadian clock, are involved in glucose homeostasis. PLoS Biol 2004;2:e377
6. Marcheva B, Ramsey KM, Buhr ED, et al. Disruption of the clock components CLOCK and BMAL1 leads to hypoinsulinaemia and diabetes. Nature 2010;466:627–631
7. Jeyaraj D, Haldar SM, Wan X, et al. Circadian rhythms govern cardiac repolarization and arrhythmogenesis. Nature 2012;483:96–99
8. Lamia KA, Storch KF, Weitz CJ. Physiological significance of a peripheral tissue circadian clock. Proc Natl Acad Sci USA 2008;105:15172–15177
9. Unger RH, Clark GO, Scherer PE, Orci L. Lipid homeostasis, lipotoxicity and the metabolic syndrome. Biochim Biophys Acta 2010;1801:209–214
10. Ando H, Yanagihara H, Hayashi Y, et al. Rhythmic messenger ribonucleic acid expression of clock genes and adipocytokines in mouse visceral adipose tissue. Endocrinology 2005;146:5631–5636
11. Zvonic S, Ptitsyn AA, Conrad SA, et al. Characterization of peripheral circadian clocks in adipose tissues. Diabetes 2006;55:962–970
12. Otway DT, Mäntele S, Bretschneider S, et al. Rhythmic diurnal gene expression in human adipose tissue from individuals who are lean, overweight, and type 2 diabetic. Diabetes 2011;60:1577–1581
13. Grimaldi B, Bellet MM, Katada S, et al. PER2 controls lipid metabolism by direct regulation of PPARγ. Cell Metab 2010;12:509–520
14. Shimba S, Ishii N, Ohta Y, et al. Brain and muscle Arnt-like protein-1 (BMAL1), a component of the molecular clock, regulates adipogenesis. Proc Natl Acad Sci USA 2005;102:12071–12076
15. Vitaterna MH, King DP, Chang AM, et al. Mutagenesis and mapping of a mouse gene, Clock, essential for circadian behavior. Science 1994;264:719–725
16. Bunger MK, Wilsbacher LD, Moran SM, et al. Mop3 is an essential component of the master circadian pacemaker in mammals. Cell 2000;103: 1009–1017
17. Yoo SH, Yamazaki S, Lowrey PL, et al. PERIOD2:LUCIFERASE real-time reporting of circadian dynamics reveals persistent circadian

oscillations in mouse peripheral tissues. Proc Natl Acad Sci USA 2004; 101:5339–5346
18. Oster H, Damerow S, Kiessling S, et al. The circadian rhythm of glucocorticoids is regulated by a gating mechanism residing in the adrenal cortical clock. Cell Metab 2006;4:163–173
19. Brown SA, Ripperger J, Kadener S, et al. PERIOD1-associated proteins modulate the negative limb of the mammalian circadian oscillator. Science 2005;308:693–696
20. Oster H, Damerow S, Hut RA, Eichele G. Transcriptional profiling in the adrenal gland reveals circadian regulation of hormone biosynthesis genes and nucleosome assembly genes. J Biol Rhythms 2006;21:350–361
21. Panda S, Antoch MP, Miller BH, et al. Coordinated transcription of key pathways in the mouse by the circadian clock. Cell 2002;109:307–320
22. Pezuk P, Mohawk JA, Yoshikawa T, Sellix MT, Menaker M. Circadian organization is governed by extra-SCN pacemakers. J Biol Rhythms 2010;25: 432–441
23. Meng QJ, McMaster A, Beesley S, et al. Ligand modulation of REV-ERBalpha function resets the peripheral circadian clock in a phasic manner. J Cell Sci 2008;121:3629–3635
24. Wu JW, Wang SP, Casavant S, Moreau A, Yang GS, Mitchell GA. Fasting energy homeostasis in mice with adipose deficiency of desnutrin/adipose triglyceride lipase. Endocrinology 2012;153:2198–2207
25. Dallmann R, Viola AU, Tarokh L, Cajochen C, Brown SA. The human circadian metabolome. Proc Natl Acad Sci USA 2012;109:2625–2629
26. Duncan RE, Ahmadian M, Jaworski K, Sarkadi-Nagy E, Sul HS. Regulation of lipolysis in adipocytes. Annu Rev Nutr 2007;27:79–101
27. Ahmadian M, Duncan RE, Sul HS. The skinny on fat: lipolysis and fatty acid utilization in adipocytes. Trends Endocrinol Metab 2009;20:424–428
28. Tsutsumi K, Inoue Y, Kondo Y. The relationship between lipoprotein lipase activity and respiratory quotient of rats in circadian rhythms. Biol Pharm Bull 2002;25:1360–1363
29. Benavides A, Siches M, Llobera M. Circadian rhythms of lipoprotein lipase and hepatic lipase activities in intermediate metabolism of adult rat. Am J Physiol 1998;275:R811–R817
30. Oishi K, Atsumi G, Sugiyama S, et al. Disrupted fat absorption attenuates obesity induced by a high-fat diet in Clock mutant mice. FEBS Lett 2006; 580:127–130
31. Kennaway DJ, Owens JA, Voultsios A, Boden MJ, Varcoe TJ. Metabolic homeostasis in mice with disrupted Clock gene expression in peripheral tissues. Am J Physiol Regul Integr Comp Physiol 2007;293:R1528–R1537
32. Guo B, Chatterjee S, Li L, et al. The clock gene, brain and muscle Arnt-like 1, regulates adipogenesis via Wnt signaling pathway. FASEB J 2012;26: 3453–3463
33. Hemmeryckx B, Himmelreich U, Hoylaerts MF, Lijnen HR. Impact of clock gene Bmal1 deficiency on nutritionally induced obesity in mice. Obesity (Silver Spring) 2011;19:659–661
34. Schweiger M, Schreiber R, Haemmerle G, et al. Adipose triglyceride lipase and hormone-sensitive lipase are the major enzymes in adipose tissue triacylglycerol catabolism. J Biol Chem 2006;281:40236–40241
35. Osuga J, Ishibashi S, Oka T, et al. Targeted disruption of hormone-sensitive lipase results in male sterility and adipocyte hypertrophy, but not in obesity. Proc Natl Acad Sci USA 2000;97:787–792
36. Haemmerle G, Lass A, Zimmermann R, et al. Defective lipolysis and altered energy metabolism in mice lacking adipose triglyceride lipase. Science 2006;312:734–737
37. Hoy AJ, Bruce CR, Turpin SM, Morris AJ, Febbraio MA, Watt MJ. Adipose triglyceride lipase-null mice are resistant to high-fat diet-induced insulin resistance despite reduced energy expenditure and ectopic lipid accumulation. Endocrinology 2011;152:48–58
38. Huijsman E, van de Par C, Economou C, et al. Adipose triacylglycerol lipase deletion alters whole body energy metabolism and impairs exercise performance in mice. Am J Physiol Endocrinol Metab 2009;297:E505–E513
39. Ahmadian M, Abbott MJ, Tang T, et al. Desnutrin/ATGL is regulated by AMPK and is required for a brown adipose phenotype. Cell Metab 2011;13: 739–748
40. Smirnova E, Goldberg EB, Makarova KS, Lin L, Brown WJ, Jackson CL. ATGL has a key role in lipid droplet/adiposome degradation in mammalian cells. EMBO Rep 2006;7:106–113
41. Zimmermann R, Strauss JG, Haemmerle G, et al. Fat mobilization in adipose tissue is promoted by adipose triglyceride lipase. Science 2004;306: 1383–1386
42. Haemmerle G, Moustafa T, Woelkart G, et al. ATGL-mediated fat catabolism regulates cardiac mitochondrial function via PPAR-α and PGC-1. Nat Med 2011;17:1076–1085
43. Oliver P, Caimari A, Díaz-Rúa R, Palou A. Diet-induced obesity affects expression of adiponutrin/PNPLA3 and adipose triglyceride lipase, two members of the same family. Int J Obes (Lond) 2012;36:225–232
44. Langin D, Dicker A, Tavernier G, et al. Adipocyte lipases and defect of lipolysis in human obesity. Diabetes 2005;54:3190–3197
45. Morimoto C, Tsujita T, Okuda H. Antilipolytic actions of insulin on basal and hormone-induced lipolysis in rat adipocytes. J Lipid Res 1998;39:957–962
46. Wang MY, Lee Y, Unger RH. Novel form of lipolysis induced by leptin. J Biol Chem 1999;274:17541–17544
47. Satoh Y, Kawai H, Kudo N, Kawashima Y, Mitsumoto A. Time-restricted feeding entrains daily rhythms of energy metabolism in mice. Am J Physiol Regul Integr Comp Physiol 2006;290:R1276–R1283
48. Eckel-Mahan KL, Patel VR, Mohney RP, Vignola KS, Baldi P, Sassone-Corsi P. Coordination of the transcriptome and metabolome by the circadian clock. Proc Natl Acad Sci USA 2012;109:5541–5546
49. Shimba S, Ogawa T, Hitosugi S, et al. Deficient of a clock gene, brain and muscle Arnt-like protein-1 (BMAL1), induces dyslipidemia and ectopic fat formation. PLoS ONE 2011;6:e25231
50. Delezie J, Dumont S, Dardente H, et al. The nuclear receptor REV-ERBα is required for the daily balance of carbohydrate and lipid metabolism. FASEB J 2012;26:3321–3335
51. Solt LA, Wang Y, Banerjee S, et al. Regulation of circadian behaviour and metabolism by synthetic REV-ERB agonists. Nature 2012;485:62–68
52. Hirota T, Lee JW, St John PC, et al. Identification of small molecule activators of cryptochrome. Science 2012;337:1094–1097
53. Hatori M, Vollmers C, Zarrinpar A, et al. Time-restricted feeding without reducing caloric intake prevents metabolic diseases in mice fed a high-fat diet. Cell Metab 2012;15:848–860
54. Barclay JL, Husse J, Bode B, et al. Circadian desynchrony promotes metabolic disruption in a mouse model of shiftwork. PLoS ONE 2012;7: e37150